Polynuclear growth model with external source and random matrix model with deterministic source

T. Imamura[1,*] and T. Sasamoto[2,†]
[1]*Department of Physics, Graduate School of Science, University of Tokyo, Hongo 7-3-1, Bunkyo-ku, Tokyo 113-0033, Japan*
[2]*Department of Physics, Tokyo Institute of Technology, Oh-okayama 2-12-1, Meguro-ku, Tokyo 152-8551, Japan*
(Received 17 November 2004; published 15 April 2005)

We present a random matrix interpretation of the distribution functions which have appeared in the study of the one-dimensional polynuclear growth (PNG) model with external sources. It is shown that the distribution, GOE^2, which is defined as the square of the Gaussian orthogonal ensemble (GOE) Tracy-Widom distribution, can be obtained as the scaled largest eigenvalue distribution of a special case of a random matrix model with a deterministic source, which have been studied in a different context previously. Compared to the original interpretation of the GOE^2 as "the square of GOE," ours has an advantage in that it can also describe the transition from the Gaussian unitary ensemble (GUE) Tracy-Widom distribution to the GOE^2. We further demonstrate that our random matrix interpretation can be obtained naturally by noting the similarity of the topology between a certain noncolliding Brownian motion model and the multilayer PNG model with an external source. This provides us with a multimatrix model interpretation of the multipoint height distributions of the PNG model with an external source.

DOI: 10.1103/PhysRevE.71.041606 PACS number(s): 81.10.Aj, 05.40.−a, 02.50.Ey, 68.55.Ac

I. INTRODUCTION

The universality of eigenvalue correlations in random matrix theory(RMT) has been arising in various fields in physics. The most recent appearance is in the one-dimensional Kardar-Parisi-Zhang(KPZ) universality class [1] which is a fundamental universality in non-equilibrium statistical mechanics. It has been found that the fluctuation of certain physical quantities in the KPZ universality class is equivalent to that of the largest eigenvalue in RMT. This fact was first pointed out in the polynuclear growth(PNG) model [2] and the totally asymmetric simple exclusion process(TASEP) [3] based on the Baik-Deift-Johansson theorem in random permutations [4].

The PNG model is a stochastic surface growth model and is the most well-understood model in the relation with RMT. Based on the results on the symmetrized random permutations [5–7], the properties of the height fluctuation of the PNG model have been analyzed for various boundary conditions. In [2] the height fluctuation of the PNG droplet in an infinite space was analyzed. It turned out that the height fluctuation is described by the GUE Tracy-Widom distribution [8]. On the other hand, in case of the growth on half line, the height fluctuation at the boundary is described by the GOE and Gaussian symplectic ensemble(GSE) Tracy-Widom distribution [9] according to the strength of an external source at the boundary [10]. Furthermore the equal time correlation of the height fluctuation at distinct points has also been analyzed for the PNG model. It has been found that it is equivalent to the process of the largest eigenvalue in the Dyson's Brownian motion model between GUEs in the case of the growth on infinite line [11,12] while in half infinite case, it corresponds to the process in the model which describes the transition between GOE/GSE and GUE [13].

In addition to the Tracy-Widom distributions for the fundamental three classes in RMT, GOE, GUE and GSE, two distribution functions, which had not been discussed in the study of RMT, arose in the description of the height fluctuation of the PNG droplet on infinite line with external sources at boundaries [10,14]. These are called F_0 and GOE^2. These functions also appear in the study of current fluctuations in TASEP [15,16]. There are also distribution functions which describe the transitions between two functions mentioned above. For instance, there is a distribution function, depending on a parameter ω, which approaches the GUE Tracy-Widom distribution as $\omega\to\infty$, tends to the Gaussian as $\omega\to-\infty$ and becomes GOE^2 when $\omega=0$. We have not yet known what kind of random matrix ensemble corresponded to F_0. The GOE^2, on the other hand, can be understood in terms of the language of RMT. It is written as the square of the GOE Tracy-Widom distribution and can be interpreted as the distribution function of the larger of the largest eigenvalues of two independent GOEs. Its Fredholm determinant representation was obtained in [17]. There, it was also shown that the scaling limit of certain eigenvalue statistics of two independent GOEs is described by its kernel.

In this paper, we present another point of view of the GOE^2 as the scaled largest eigenvalue distribution of a random matrix with a deterministic source. The advantage of this ensemble is that it can describe the GUE-GOE^2 transition in the PNG model, which is induced by the change of the external source while this transition cannot be obtained by the measure of "the square of GOE."

From the point of view of the PNG model with external sources, our viewpoint is more natural than that of "the square of GOE." We turn our attention on the topology and the structure of the determinantal measure in the multilayer version of the PNG model with an external source. Our ran-

*Email address: imamura@monet.phys.s.u-tokyo.ac.jp
†Email address: sasamoto@stat.phys.titech.ac.jp

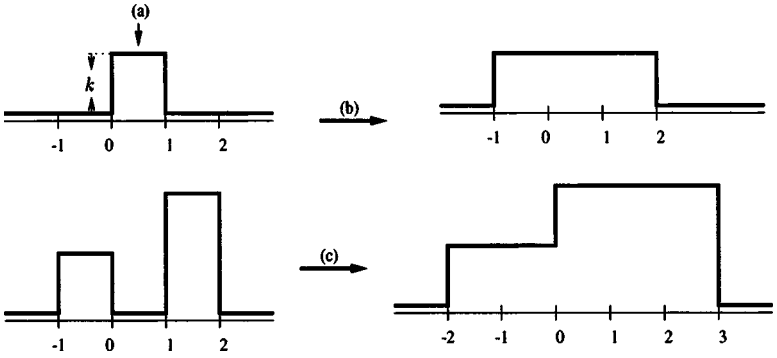

FIG. 1. Rules of the discrete PNG model. Here we draw the solid lines using $h([r],t)$.

dom matrix ensemble is obtained by noticing that a certain type of the noncolliding Brownian motion has a similar topology and the structure of the measure.

The random matrix obtained in this paper is a special case of the random matrix with a deterministic source, which has been studied in [18–26]. In a special case, which is different from ours, its eigenvalue statistics has an interesting property that the level spacing distribution becomes an intermediate one between the Poisson and the Wigner-Dyson statistics. This property connects it with the fields in physics such as the quantum chaos, the metal-insulator transition in disordered systems and so on. Recently the universality of such eigenvalue statistics in this model have been analyzed by the Riemann-Hilbert technique [27–30].

This paper is arranged as follows. In the next section we summarize the results on the height distribution in the PNG model with an external source. Then we introduce a random matrix with a deterministic source and compare its largest eigenvalue statistics with the height fluctuation of the PNG model. In Sec. III we consider a reason why such a random matrix model appears in the context of the PNG model with an external source. We notice that the multilayer version of the PNG model can be regarded as a noncolliding many body random walks (vicious walk) and hence inherits a free fermionic picture. By considering a certain vicious walk which is expected to have a similar property to the multilayer PNG model, we see there appears naturally a Dyson's Brownian motion model (a multimatrix model) involving an external source in the initial condition. Finally we show the equal-time correlation of the PNG model with an external source is equivalent to the dynamical correlations of the largest eigenvalue in the Dyson's Brownian motion model. The last section is devoted to the conclusion.

II. PNG MODEL AND RANDOM MATRIX WITH DETERMINISTIC SOURCE

A. PNG model with external source

First of all we give the definition of the one-dimensional discrete PNG model [12]. Let $r \in \{\ldots,-1,0,1,\ldots\}$ and $t \in \{1,2,\ldots\}$ be the space and time coordinate, respectively. The model is a stochastic surface growth model and consists of the rules (a)–(c). Figure 1 illustrates these rules.

(a) At time t, a nuclear is generated randomly at $r=-t+1,-t+3,\ldots,t-3,t-1$. The height $k(=0,1,2,\ldots)$ of each nuclear is independent of r and obeys the geometric distribution with some parameter which is fixed shortly. This is called nucleation. While a nucleation is stochastic, a growth after the nucleation given by the rules (b) and (c) is deterministic.

(b) Each nuclear grows laterally with one step toward right and left at each time step and then forms a step.

(c) When a step crashes against another step, the height of the crashing point is that of the higher one.

These rules (a)–(c) can be formulated by a single equation,

$$h(r,t+1) = \max[h(r-1,t), h(r,t)h(r+1,t)] + \omega(r,t+1). \tag{2.1}$$

Here $h(r,t)$ is the height of the surface at time t and at position r, and $\omega(r,t)$ means a height of a nucleation which is a random variable.

In this paper we set the random variable $\omega(r,t)$ as follows.

$$\begin{cases} \text{When } t-|r|>0 \text{ and } t-r \text{ is odd,} \\ \quad \mathbb{P}[\omega(r,t)=k] = \begin{cases} (1-\alpha\sqrt{q})(\alpha\sqrt{q})^k, & r=-t+1, \\ (1-q)q^k, & \text{otherwise.} \end{cases} \\ \text{Otherwise} \\ \quad \omega(r,t)=0. \end{cases} \tag{2.2}$$

Because of the condition that the nucleation occurs only when $t-|r|>0$, the surface grows into a droplet shape. The condition that $t-r$ is odd is imposed only for a technical reason and is irrelevant to the physical properties. Basically $\omega(r,t)$ is a geometric random variable with a parameter q. Only on the left edge, the parameter is $\alpha\sqrt{q}(\sqrt{q} \leqslant \alpha < 1/\sqrt{q})$. Thus the parameter α adjusts the boundary condition as an external source. This situation representing (2.2) is depicted in Fig. 2.

In the setting of (2.1) and (2.2), we focus on the distribution of the scaled height at the origin H_N defined as

$$H_N = \frac{h(r=0,t=2N)-aN}{dN^{1/3}}, \tag{2.3}$$

where $a=2\sqrt{q}/(1-\sqrt{q})$, $d=(1+\sqrt{q})^{1/3}q^{1/6}/(1-\sqrt{q})$. The limiting distribution has been obtained in [2,10,14]. It depends dramatically on the value of α. The result is

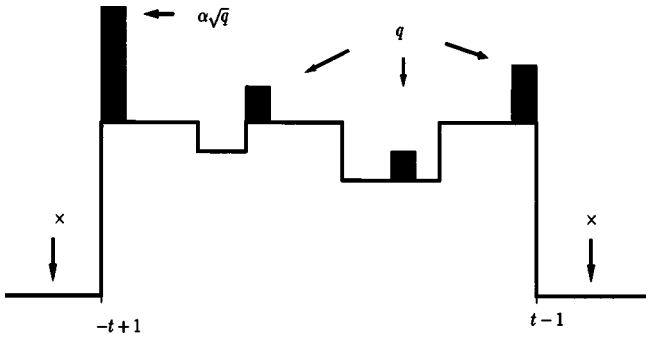

FIG. 2. Typical situation in the PNG droplet with an external source. In this model the rate of growth at the left edge ($r=-t+1$) is higher than that at other places since the parameter of a nucleation at the left edge, $\alpha\sqrt{q}$, is larger than that at other points, q.

$$\lim_{N\to\infty}\mathbb{P}[H_N\leqslant s]=\begin{cases}F_2(s), & \text{for } \sqrt{q}\leqslant\alpha<1,\\ F_1(s)^2, & \text{for } \alpha=1,\\ 0, & \text{for } 1<\alpha<\dfrac{1}{\sqrt{q}},\end{cases} \tag{2.4}$$

where $F_2(s)$ and $F_1(s)$ are the GUE and GOE Tracy-Widom distribution, respectively [8,9]. $F_2(s)$ is defined as follows. Let λ_1 be the largest eigenvalue in $N\times N$ GUE random matrix with the measure

$$e^{-\mathrm{tr}M_2^2}dM_2, \tag{2.5}$$

where M_2 is an $N\times N$ Hermitian matrix. Taking the edge scaling for λ_1,

$$\lambda_1=\sqrt{2N}+\frac{X_1}{\sqrt{2}N^{1/6}}, \tag{2.6}$$

we define $F_2(s)$ as the limiting distribution of X_1,

$$F_2(s)\equiv\lim_{N\to\infty}\mathbb{P}[X_1\leqslant s]. \tag{2.7}$$

$F_1(s)$ is also defined in the same way as above for $N\times N$ GOE random matrix with the measure

$$e^{-\mathrm{tr}M_1^2/2}dM_1, \tag{2.8}$$

where M_1 is an $N\times N$ real symmetric matrix. Hence the distribution $F_1(s)^2$, can be interpreted as the distribution of the largest eigenvalue in the superimposition of eigenvalues of two independent GOE random matrices. In this sense the distribution defined by $F_1(s)^2$ is denoted as GOE^2.

Both $F_2(s)$ and $F_1(s)^2$ can be represented as the Fredholm determinant,

$$F_2(s)=\det[1+\mathcal{K}_2 g],\quad F_1(s)^2=\det[1+\mathcal{K}_{12}g], \tag{2.9}$$

where $g(x)=-\chi_{(s,\infty)}(x)$. The definition of the Fredholm determinant with kernel $\mathcal{K}(x,y)$ is

$$\det[1+\mathcal{K}g]=\sum_{k=0}^{\infty}\frac{1}{k!}\int_{-\infty}^{\infty}\cdots\int_{-\infty}^{\infty}dx_1\cdots dx_k g(x_1)\cdots g(x_k)\times\det[\mathcal{K}(x_i,x_j)]_{i,j=1}^{k}. \tag{2.10}$$

The kernels $\mathcal{K}_2(x,y)$ and $\mathcal{K}_{12}(x,y)$ have the following form:

$$\mathcal{K}_2(x,y)=\int_0^{\infty}d\sigma\,\mathrm{Ai}(x+\sigma)\mathrm{Ai}(y+\sigma),$$

$$\mathcal{K}_{12}(x,y)=\mathcal{K}_2(x,y)+\mathrm{Ai}(x)\int_0^{\infty}d\sigma\,\mathrm{Ai}(y-\sigma). \tag{2.11}$$

Here $\mathcal{K}_2(x,y)$ is called the Airy kernel [31] and $\mathcal{K}_{12}(x,y)$ is obtained in [17].

Thus, when $\alpha\leqslant 1$, the result (2.4) can be rewritten as

$$\lim_{N\to\infty}\mathbb{P}[H_N\leqslant s]=\det[1+\mathcal{K}g], \tag{2.12}$$

where

$$\mathcal{K}(x,y)=\begin{cases}\mathcal{K}_2(x,y)=\displaystyle\int_0^{\infty}d\sigma\,\mathrm{Ai}(x+\sigma)\mathrm{Ai}(y+\sigma), & \text{for } \sqrt{q}\leqslant\alpha<1,\\ \mathcal{K}_{12}(x,y)=\mathcal{K}_2(x,y)+\mathrm{Ai}(x)\displaystyle\int_0^{\infty}d\sigma\,\mathrm{Ai}(y-\sigma), & \text{for } \alpha=1.\end{cases} \tag{2.13}$$

When $1<\alpha<1/\sqrt{q}$, the result (2.4) that the limiting distribution vanishes implies that we have to define another scaled height,

$$H_N^{(G)}=\frac{h(r=0,t=2N)-a_G N}{d_G N^{1/2}}, \tag{2.14}$$

where $a_G=q^{1/2}(1-2\alpha q^{1/2}+\alpha^2)/(\alpha-q^{1/2})(1-\alpha q^{1/2})$ and $d_G=\alpha^{1/2}q^{1/4}(1-q)^{1/2}(\alpha^2-1)^{1/2}/(1-\alpha q^{1/2})(\alpha-q^{1/2})$. Then the limiting distribution becomes the error function,

$$\lim_{N\to\infty}\mathbb{P}[H_N^{(G)}\leqslant s]=\frac{1}{\sqrt{2\pi}}\int_{-\infty}^{s}d\xi\,e^{-\xi^2/2},\quad \text{for } 1<\alpha<\frac{1}{\sqrt{q}}. \tag{2.15}$$

B. Random matrix with deterministic source

When we look at the above results, we notice a fact that the distribution at $\alpha=1$, which we call GOE^2, appears in the intertwining point between Gaussian statistics and RMT statistics. First, let us consider the distribution of the height at the origin when α is extremely large. In this case we can easily expect that it is the Gaussian since the height at the origin is virtually determined by nucleations at the only one point, the left edge due to the rule (b). Equation (2.15) confirms this discussion. When $\alpha=\sqrt{q}$, on the other hand, it is described by the GUE Tracy-Widom distribution as discussed above. The GOE^2 arises in the situation where these two statistics compete, i.e., when $\alpha=1$.

Considering this property, we introduce a simple random matrix model which is expected to describe the GUE random matrix–Gaussian transition of the largest eigenvalue. We consider a random matrix H_0 defined as

$$H_0 = H + V, \tag{2.16}$$

where H is the GUE random matrix and V is the deterministic diagonal matrices, $V=\mathrm{diag}(\epsilon_j)$ $(j=1,\ldots,N)$. The measure can be defined as

$$e^{-\mathrm{tr}H^2} dH_0. \tag{2.17}$$

Focusing on the case where

$$\epsilon_1 = \epsilon, \epsilon_2 = \cdots = \epsilon_N = 0, \tag{2.18}$$

we can expect that when ϵ is sufficiently large the largest eigenvalue is isolated from others by the effect of ϵ and then the fluctuation becomes the Gaussian while this becomes the GUE Tracy-Widom distribution when ϵ is sufficiently small.

The eigenvalue statistics of (2.16) and (2.17) is analyzed in [18–26]. For the distribution of the largest eigenvalue λ_1, their results lead to the Fredholm determinant expression,

$$\mathbb{P}[\lambda_1 \leqslant s] = \det[1 + K_N g]. \tag{2.19}$$

Here the kernel $K_N(x,y)$ can be expressed as a double integral,

$$K_N(x,y) = -\int_\Gamma \frac{dv}{2\pi i}\int \frac{du}{2\pi}\prod_{j=1}^{N}\left[\frac{-\epsilon_j - \frac{iu}{2}}{v-\epsilon_j}\right]\frac{e^{-u^2/4-v^2+iux+2vy}}{v+i\frac{u}{2}}, \tag{2.20}$$

where Γ denotes a contour enclosing $\{\epsilon_j\}_{j=1,\cdots,N}$ anticlockwise and the integration with respect to u is taken from $-\infty$ to ∞ and not to cross Γ.

In this formula with the condition (2.18), we consider the following scaling limit,

$$x = \sqrt{2N} + \frac{X}{\sqrt{2}N^{1/6}}, \quad y = \sqrt{2N} + \frac{Y}{\sqrt{2}N^{1/6}}, \quad \epsilon = \Lambda\sqrt{\frac{N}{2}}, \tag{2.21}$$

with $\Lambda(\leqslant 1)$ fixed. This corresponds to the edge scaling limit (2.6) of the eigenvalues. Applying the saddle point method, the limiting kernel can be calculated. The result depends on the value of Λ,

$$K_N(x,y) \rightharpoonup \begin{cases} \mathcal{K}_2(X,Y) = \displaystyle\int_0^\infty d\sigma\, \mathrm{Ai}(X+\sigma)\mathrm{Ai}(Y+\sigma), & \text{for } \Lambda < 1, \\ \mathcal{K}_{12}(X,Y) = \mathcal{K}_2(X,Y) + \mathrm{Ai}(X)\displaystyle\int_0^\infty d\sigma\, \mathrm{Ai}(Y-\sigma), & \text{for } \Lambda = 1. \end{cases} \tag{2.22}$$

Note that the kernel (2.22) is exactly the same as that in the PNG model with an external source (2.13) and Λ, the parameter of the deterministic source in RMT corresponds to α, the parameter of the external source in PNG model. Hence we find that the height fluctuation in the PNG model with an external source shares the limiting distribution with the largest eigenvalue fluctuation of the random matrix with deterministic source defined in (2.16)–(2.18). The same distributions appear in the distribution of the largest eigenvalue of the non-null complex sample covariance matrices [32].

When $\Lambda>1$ in (2.21), we change the edge scaling (2.21) to

$$x = A_G N^{1/2} + B_G X, \quad y = A_G N^{1/2} + B_G Y, \tag{2.23}$$

where $A_G=(1/\sqrt{2})(\Lambda+1/\Lambda)$ and $B_G=\sqrt{(\Lambda^2-1)/2\Lambda^2}$. The kernel is asymptotically

$$K_N(x,y) \sim \mathcal{K}_G(X,Y) = \frac{e^{\sqrt{2N}\Lambda(y-x)}}{\sqrt{2\pi}B_G} e^{-x^2/2}, \quad \text{for } \Lambda > 1. \tag{2.24}$$

Thus we get

$$\lim_{N\to\infty}\mathbb{P}\left[\frac{\lambda_1 - A_G\sqrt{N}}{B_G} \leqslant s\right] = \frac{1}{\sqrt{2\pi}}\int_{-\infty}^{s} d\xi\, e^{-\xi^2/2}. \tag{2.25}$$

This result corresponds to (2.15). Note that the factor $e^{\sqrt{2N}\Lambda(y-x)}$ in (2.24) does not contribute to the Fredholm determinant.

At last we give a proof of (2.24). The main result in this section (2.22) will be derived in Sec. III D under a more general situation.

Rescaling the variables in (2.20) under the condition (2.18) such that

$$v = \sqrt{\frac{N}{2}}z, \quad -\frac{iu}{2} = \sqrt{\frac{N}{2}}w, \quad \epsilon = \Lambda\sqrt{\frac{N}{2}}, \tag{2.26}$$

one finds

$$K_N(x,y) = \frac{\sqrt{2N}}{(2\pi i)^2}\int_{\Gamma'} dz \int_{-i\infty}^{i\infty} dw \frac{z}{w}\frac{w-\Lambda}{z-\Lambda}\frac{1}{w-z} \times \frac{e^{(\sqrt{2N}y-\sqrt{2}A_G N)z}}{e^{(\sqrt{2N}x-\sqrt{2}A_G N)w}} e^{N\{f_G(w)-f_G(z)\}}, \tag{2.27}$$

where the contour Γ' encloses the origin and Λ anticlockwise and

$$f_G(w) = \frac{w^2}{2} - \sqrt{2}A_G w + \ln w. \tag{2.28}$$

$K_N(x,y)$ can be divided into two parts,

$$K_N(x,y) = K_N^{(1)}(x,y) + K_N^{(2)}(x,y). \tag{2.29}$$

Here $K_N^{(1)}$ and $K_N^{(2)}$ correspond to a contour integral of z around Λ and the origin respectively and have the forms

$$K_N^{(1)}(x,y) \equiv \frac{\sqrt{2N}\Lambda}{2\pi i}\frac{e^{(\sqrt{2N}y-\sqrt{2}A_G N)\Lambda}}{e^{Nf_G(\Lambda)}} e^{-Nf_G(\Lambda)} \times \int_{-i\infty}^{i\infty} \frac{dw}{w}\frac{e^{Nf_G(w)}}{e^{(\sqrt{2N}x-\sqrt{2}A_G N)w}}, \tag{2.30}$$

$$K_N^{(2)}(x,y) \equiv \frac{\sqrt{2N}}{(2\pi i)^2}\oint dz \int_{-i\infty}^{i\infty} dw \frac{z}{w}\frac{w-\Lambda}{z-\Lambda}\frac{1}{w-z} \times \frac{e^{(\sqrt{2N}y-\sqrt{2}A_G N)z}}{e^{(\sqrt{2N}x-\sqrt{2}A_G N)w}} e^{N\{f_G(w)-f_G(z)\}}, \tag{2.31}$$

where $\oint$ means the contour enclosing the origin anticlockwise. We analyze the asymptotic form of each $K_N^{(i)}(i=1,2)$ by the saddle point method under the scaling (2.23).

At first we consider $K_N^{(1)}(x,y)$. We deform the path of integration of w to the one which passes a critical point $w_c = \Lambda$ of $f_G(w)$. We set

$$w = \Lambda + \frac{iw_1}{\sqrt{2NB_G}} \tag{2.32}$$

and substitute this into the integrand in (2.30) to get

$$Nf_G(w) \sim Nf_G(\Lambda) - \frac{w_1^2}{2},$$

$$e^{(\sqrt{2N}x-\sqrt{2}A_G N)w} \sim e^{(\sqrt{2N}x-\sqrt{2}A_G N)\Lambda} e^{iw_1 X}. \tag{2.33}$$

Thus one finds

$$K_N^{(1)} \sim e^{\sqrt{2N}\Lambda(y-x)}\frac{e^{-X^2/2}}{\sqrt{2\pi}B_G}. \tag{2.34}$$

For $K_N^{(2)}(x,y)$, we deform the path of the variable z in a way that it crosses another critical point $z_c = 1/\Lambda$ of $f_G(z)$ while as for w, we again use (2.32). Hence z is transformed to

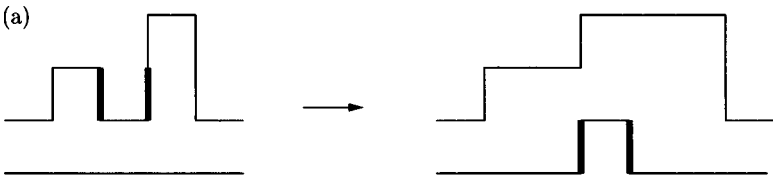

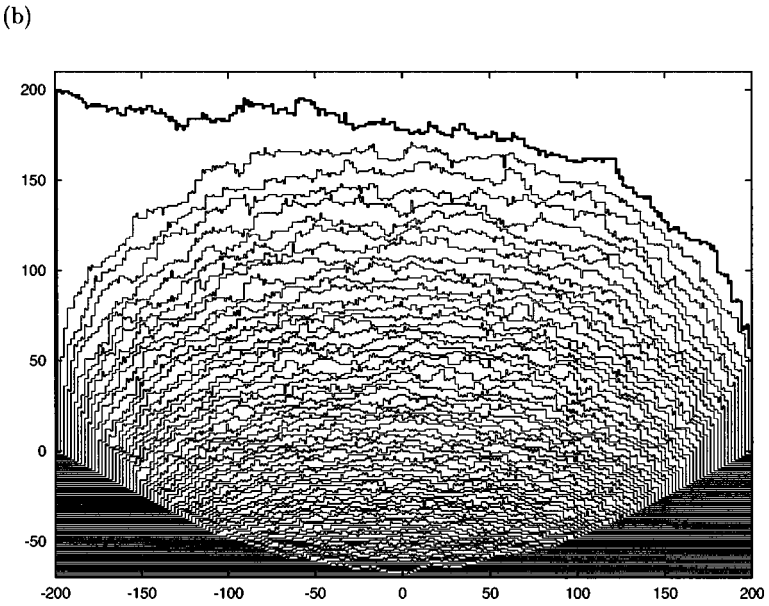

FIG. 3. (a) Rule of the multilayer PNG model. Due to the rule(c) of the PNG model, the part illustrated by the thick lines vanishes in the first layer. This part, however, is recovered by the nucleation of the layer below. For the second and subsequent layers, we follow the same procedure. (b) A typical configuration of the PNG droplet with an external source for $\alpha=1$, $q=\frac{1}{4}$, and $t=200$.

$$z = \frac{1}{\Lambda} + \frac{iw_2}{\sqrt{2NB_G}}, \tag{2.35}$$

and then we get

$$\begin{aligned} -Nf_G(z) &\sim -Nf_G\left(\frac{1}{\Lambda}\right) - \frac{w_1^2}{2}, \\ e^{(\sqrt{2N}y-\sqrt{2}A_G N)z} &\sim e^{(\sqrt{2N}y-\sqrt{2}A_G N)/\Lambda} e^{iw_2 Y}. \end{aligned} \tag{2.36}$$

Due to (2.33) and (2.36), one finds

$$\begin{aligned} K_N^{(2)}(x,y) &\sim e^{N\{f_G(\Lambda)-f_G(1/\Lambda)\}} e^{O(N^{1/2})} \\ &= e^{-(N/2)(\Lambda^2-1/\Lambda^2-4\ \mathrm{In}\Lambda)} e^{O(N^{1/2})} \to 0, \end{aligned} \tag{2.37}$$

where we use $\Lambda > 1$.

Thus from (2.29), (2.34), and (2.37), we finally get (2.24).

III. FREE FERMIONIC PICTURE

A. Multilayer PNG

In the above section we discussed the limiting distribution of the scaled height at the origin in the PNG model and its dependence on the external source. In the next step, we would like to consider the multipoint equal time joint distributions. To do this, we introduce the multilayer PNG model from the time evolution of the PNG model [11,12].

The rule of the multilayer PNG model is as follows. When two steps collide, the lower step is absorbed by the higher one due to the rule (c). We recover this absorbed height as the nucleation in the layer below. This situation and a typical example of the multilayer PNG model are illustrated in Fig. 3. Note that the first layer of the multilayer PNG model represents the shape of the PNG droplet while other layers record the time evolution of the growth.

If we treat the ith layer of the multilayer PNG model as the ith random walker, the multilayer PNG model can be regarded as a noncolliding random walks called the vicious walk. Thus the multipoint equal time correlation of the PNG model, which is our target, corresponds to the dynamical correlation of the first walker in the noncolliding random walks. Note that we treat the space axis in the PNG model as the time axis in the point of view of the vicious walk. The advantage of the mapping is that as we will see below, the measure can be described in the form of products of determinants. This determinantal structure is associated with the structure of wavefunction in the N-body free fermions, i.e., the Slater determinant.

In [33], we could obtain the multipoint equal time joint distributions in the PNG model having external sources at both edges by introducing the multilayer PNG model. The result specialized to the case considered here is the following.

We define the scaled height $H_N(\tau)$ near the origin as

$$H_N(\tau) = \frac{h(2cN^{2/3}\tau, t = 2N) - aN}{dN^{1/3}} + \tau^2, \tag{3.1}$$

where a and d are already given below (2.3) and $c=(1+\sqrt{q})^{2/3}/q^{1/6}$. We set the parameter of the external source as

$$\alpha = 1 - \frac{\omega}{dN^{1/3}}. \tag{3.2}$$

The equal time multipoint distribution function near the origin is described by the Fredholm determinant,

$$\begin{aligned} &\lim_{N\to\infty} \mathbb{P}[H_N(\tau_1) \leqslant s_1, \ldots, H_N(\tau_m) \leqslant s_m] \\ &\quad = \det[1 + \mathcal{K}\mathcal{G}], \\ &\quad \equiv \sum_{k=0}^{\infty} \frac{1}{k!} \sum_{n_1=1}^{m} \int_{-\infty}^{\infty} d\xi_1 \cdots \sum_{n_k=1}^{m} \int_{-\infty}^{\infty} d\xi_k \mathcal{G}(\tau_{n_1}, \xi_1) \cdots \mathcal{G}(\tau_{n_k}, \xi_k) \\ &\quad \times \det[\mathcal{K}(\tau_{n_l}, \xi_l; \tau_{n_{l'}}, \xi_{l'})]_{l,l'=1}^{k}, \end{aligned} \tag{3.3}$$

where $\mathcal{G}(\tau_j, \xi) = -\chi_{(s_j,\infty)}(\xi) (j = 1, 2, \ldots, m)$. The kernel is

$$\begin{aligned} \mathcal{K}(\tau_1, \xi_1; \tau_2, \xi_2) &= \mathcal{K}_2^{\mathrm{ext}}(\tau_1, \xi_1; \tau_2, \xi_2) \\ &\quad + \mathrm{Ai}(\xi_1) \int_0^{\infty} d\lambda\, e^{-(\omega+\tau_2)\lambda} \mathrm{Ai}(\xi_2 - \lambda), \end{aligned} \tag{3.4}$$

where

$$\mathcal{K}_2^{\mathrm{ext}}(\tau_1, \xi_1; \tau_2, \xi_2) = \begin{cases} \displaystyle\int_0^{\infty} d\lambda\, e^{-\lambda(\tau_1-\tau_2)} \mathrm{Ai}(\xi_1 + \lambda) \mathrm{Ai}(\xi_2 + \lambda), & \tau_1 \geqslant \tau_2, \\ \displaystyle -\int_{-\infty}^{0} d\lambda\, e^{-\lambda(\tau_1-\tau_2)} \mathrm{Ai}(\xi_1 + \lambda) \mathrm{Ai}(\xi_2 + \lambda), & \tau_1 < \tau_2. \end{cases} \tag{3.5}$$

In the case where all $\tau_i = 0$, another representation of this distribution has been obtained via Riemann-Hilbert method by Baik and Rains [14].

The kernel $\mathcal{K}_2^{\mathrm{ext}}$ is called the extended Airy kernel [34] and the process described by this Fredholm determinant is called the Airy process [11,12]. It describes the process of the largest eigenvalue in the Dyson's Brownian motion model in Hermitian matrices. It also describes the correlation function of the PNG model without an external source.

Looking at the correlation function (3.3) at one point case ($m=1$), we can find that it expresses the GOE^2-GUE transition induced by both parameters of the external source ω and a position τ. Setting $\omega=\tau_1=0$ in (3.4) in the one point case, we get $\mathcal{K}=\mathcal{K}_{12}$ which is the kernel of the edge scaling in GOE^2 ensemble while in the case where $\omega\to\infty$ or $\tau\to\infty$ one finds $\mathcal{K}\sim\mathcal{K}_2$ and the GUE case is recovered.

B. Noncolliding Brownian motion and multimatrix model

In Sec. II B the random matrix with a deterministic source, which corresponds to the PNG model with an external source was introduced from an intuitive argument. Here we show that the measure of the random matrix with a deterministic source is obtained naturally by considering the measure of the multilayer version of the PNG model with an external source. The analysis not only reproduces the result in Sec. II B but also provides a multimatrix model which has the kernel (3.4) in the edge scaling limit.

As was shown in the above subsection, it is found through the multilayer PNG model that the structure of the vicious walk (free-fermionic structure) is hidden in the measure of the PNG model. Particularly we focus on the two properties in the measure of the vicious walk. The first property is the determinantal structure which the vicious walk and RMT share. The second one is the topology of the vicious walk. In our case, Fig. 3(b), the top layer, which corresponds to the top walker in the point of view of the vicious walk, seem to start from the point far from the other walkers due to the effect of the external source. In the study of vicious walks, it has been known that in some cases the measure can be represented as that of a multimatrix model in an appropriate scaling limit and its topology determines the universality classes of the measure in RMT [35,36].

Keeping in mind the above two properties, we begin our discussion with writing down the measure of noncolliding Brownian motion which can be regarded as the continuous limit of the vicious walk. Let $x_r^{(j)}(r=1,\ldots,N, j=0,\ldots,M+1)$ be the position of rth walker from top at the time labeled by j. By the Karlin-McGregor theorem, the measure that the walkers have a configuration $\{x_r^{(j)}\}$ is obtained as a product of the determinants of propagators of the one-body Brownian motion,

$$\frac{1}{Z}\prod_{j=0}^{M}\det\left[\psi_{j,j+1}(x_r^{(j)},x_s^{(j+1)})\right]_{r,s=1}^{N}. \tag{3.6}$$

Here Z is the normalization constant and $\psi_{j,j+1}(x_r^{(j)},x_s^{(j+1)})$ is the propagator of the one body Brownian motion from $x_r^{(j)}$ to $x_s^{(j+1)}$ with interval T_j,

$$\psi_{j,j+1}(x_r^{(j)},x_s^{(j+1)})=\frac{1}{\sqrt{2\pi T_j}}\exp\left\{-(x_s^{(j+1)}-x_r^{(j)})^2/2T_j\right\}. \tag{3.7}$$

Then we take the following scaling limit:

$$T_j=r_jT(j=0,1,2,\ldots,M),\quad x_r^{(j)}=\begin{cases}\dfrac{\sqrt{T}\epsilon_r}{2}, & j=0,\\ \sqrt{s_jT}\lambda_r^{(j)}, & j=1,2,\ldots,M,\\ b_r, & j=M+1.\end{cases} \tag{3.8}$$

Note that if we take the parameter of the initial condition to be $\epsilon_1=\epsilon$, $\epsilon_2=\cdots=\epsilon_N=0$, the topology of the configuration becomes similar to that in the multilayer PNG model with an external source. (See Fig. 4.) Substituting (3.8) to (3.7), we get

$$\frac{1}{Z}\prod_{j=0}^{M}\det[\psi_{j,j+1}(x_r^{(j)},x_s^{(j+1)})]=\frac{W_T[\lambda^{(1)},\ldots,\lambda^{(M)}]}{Z'}, \tag{3.9}$$

where Z' is the normalization constant. The weight W_T has the following form,

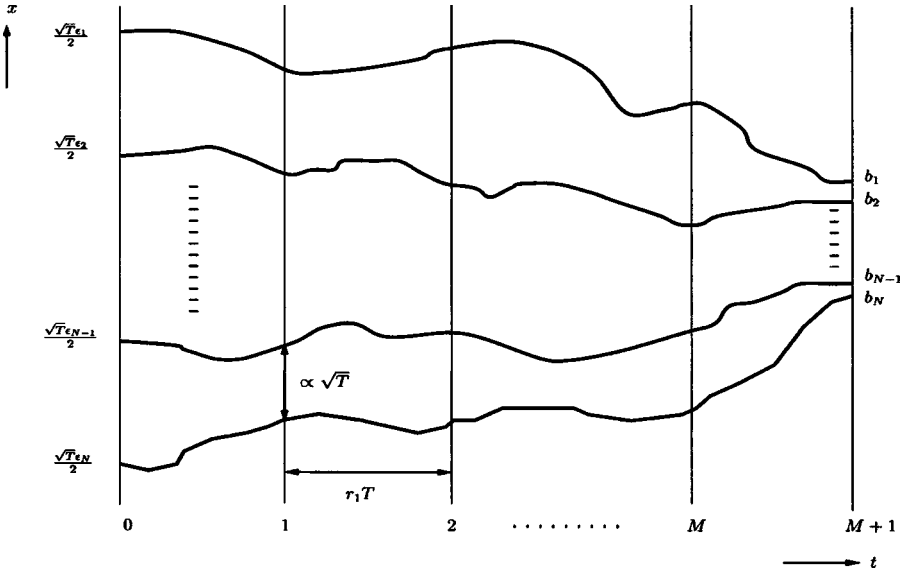

FIG. 4. Noncolliding Brownian motion in the scaling limit (3.8).

$$W_T[\lambda^{(1)},\ldots,\lambda^{(M)}] = \prod_{j=1}^{M}\prod_{r=1}^{N} e^{-V_j(\lambda_r^{(j)})} \prod_{j=1}^{M-1} \det[e^{c_j\lambda_r^{(j)}\lambda_s^{(j+1)}}] \times \frac{\det[e^{c_0\epsilon_r\lambda_s^{(1)}}]}{\Delta(\epsilon)} \det\left[e^{(\sqrt{s_M}/r_M\sqrt{T})\lambda_r^{(M)}b_s}\right], \tag{3.10}$$

where $\lambda^{(i)}$ means $\{\lambda_r^{(i)}\}_{r=1,\ldots,N}$ and

$$V_j(x) = \frac{s_j}{2}\left(\frac{1}{r_{j-1}} + \frac{1}{r_j}\right)x^2, \quad c_j = \frac{\sqrt{s_j s_{j+1}}}{r_j}, \quad c_0 = \frac{\sqrt{s_1}}{2r_0},$$

$$\Delta(x) = \prod_{i<j}^{N} |x_i - x_j|. \tag{3.11}$$

In (3.10), we include the term $\Delta(\epsilon)$ in order to get a finite expression when we consider the special case where (2.18) in the later discussion. Applying to the last term in W_T the following formula,

$$\lim_{\{z_i\}\to 1} \frac{\det\left[z_i^{\xi_j+N-j}\right]}{\det\left[z_i^{N-j}\right]} = \prod_{1\le i<j\le N} \frac{\xi_i - \xi_j + j - i}{j-i}, \tag{3.12}$$

where $\{\xi_i\}\in\mathbb{C}^{\mathbb{N}}$, one finds for large T,

$$\det\left[e^{(\sqrt{s_M}/r_M\sqrt{T})\lambda_r^{(M)}b_s}\right] = \frac{\det\left[e^{(\sqrt{s_M}/r_M\sqrt{T})\lambda_r^{(M)}b_s}\right]}{\det\left[\left(e^{\lambda_i^{(M)}/\sqrt{T}}\right)^{N-j}\right]} \det\left[\left(e^{\lambda_j^{(M)}/\sqrt{T}}\right)^{N-j}\right] \sim \prod_{1\le i<j\le N} \frac{\sqrt{s_M}(b_i - b_j)}{j-i} \frac{\Delta(\lambda^{(M)})}{T^{N(N-1)/4}}. \tag{3.13}$$

Thus we get

$$\lim_{T\to\infty} \frac{W_T}{Z'} = \frac{1}{Z''}\prod_{j=1}^{M}\prod_{r=1}^{N} e^{-V_j(\lambda_r^{(j)})} \prod_{j=1}^{M-1} \det[e^{c_j\lambda_r^{(j)}\lambda_s^{(j+1)}}] \times \frac{\det[e^{c_0\epsilon_r\lambda_s^{(1)}}]}{\Delta(\epsilon)} \Delta(\lambda^{(M)}). \tag{3.14}$$

Up to a trivial constant, (3.14) is equivalent to the weight of the eigenvalues of the Hermitian multimatrix model,

$$\prod_{j=1}^{M} e^{-\mathrm{tr}V_j(H_j)} \prod_{j=1}^{M-1} e^{\mathrm{tr}c_j H_j H_{j+1}} e^{\mathrm{tr}c_0 V H_1} dH_1\cdots dH_M. \tag{3.15}$$

Here $H_j (j=1,\ldots,M)$ is an $N\times N$ Hermitian matrix and $V=\mathrm{diag}(\epsilon)$. This equivalence can be shown through the Harish-Chandra, Itzykson-Zuber integral [37,38],

$$\int dU \exp(\mathrm{tr}\, AUBU^{\dagger}) \propto \frac{\det[\exp(a_i b_j)]}{\Delta(a)\Delta(b)}, \tag{3.16}$$

where U is $N\times N$ unitary matrix, dU is the Haar measure and A and B are $N\times N$ Hermitian matrices with eigenvalues a_i and b_i respectively. Note than in the case of one matrix model, (3.15) is the same form as the random matrix with deterministic source (2.16) and (2.17) discussed in Sec. II. We further transform the variables s_j and r_j as

$$s_j = e^{2t_j}, \quad r_j = \frac{1 - e^{2(t_j - t_{j+1})}}{2e^{-2t_{j+1}}}, \quad r_0 = 1/2, \quad r_M \to \infty, \tag{3.17}$$

with $t_1=0$. Then one finds (3.15) can be represented as the form of Dyson's Brownian motion model,

$$\prod_{j=1}^{M-1} \exp\left[\frac{-\mathrm{tr}\{H_{j+1} - e^{t_j - t_{j+1}}H_j\}^2}{1 - e^{2(t_j - t_{j+1})}}\right] \times \exp[-\mathrm{tr}H_1^2 + \mathrm{tr}VH_1] dH_1\cdots dH_M. \tag{3.18}$$

C. Dynamical correlation function

In the above discussion we construct the Dyson's Brownian motion model with the deterministic source from the noncolliding Brownian motion with the topology appropriate to the multilayer PNG model with an external source. Next we would like to analyze the process of the largest eigenvalue of this model since it corresponds to the equal time correlation of the height distribution in the PNG model.

The measure for the eigenvalues in (3.18) is

$$\prod_{j=1}^{M-1} \det[\phi(t_j,\lambda_r^{(j)};t_{j+1},\lambda_s^{(j+1)})]_{r,s=1}^{N} e^{\sum_j -(\lambda_j^{(1)})^2} \times \det[e^{\epsilon_j\lambda_k^{(1)}}]_{j,k=1}^{N} \det[(\lambda_j^{(M)})^k]_{k=0,\ldots,N-1}^{j=1,\ldots,N}, \tag{3.19}$$

where we denote the eigenvalue for the matrix H_j as $\{\lambda_k^{(j)}\}_{k=1,\ldots,N}$

$$\varphi(t_i,x;t_j,y) = \begin{cases} \sqrt{\dfrac{e^{t_i-t_j}}{\pi(1-e^{2(t_i-t_j)})}} \exp\left[-\dfrac{(y - e^{t_i-t_j}x)^2}{1-e^{2(t_i-t_j)}}\right], & \text{for } t_i \le t_j, \\ 0, & \text{for } t_i > t_j. \end{cases} \tag{3.20}$$

Under this measure, we focus on the following probability:

$$\mathbb{P}[\lambda_1^{(1)} \le s_1,\ldots,\lambda_1^{(M)} \le s_M]. \tag{3.21}$$

We analyze this quantity by following the strategy of Johansson [12] although we can caluclate it also by the method of Brézin-Hikami [19] with some effort.

In [12] it is shown that the correlation function (3.21) can be expressed as the Fredholm determinant for the case where the measure is given in the determinantal form such as (3.19) by generalizing the method of Tracy-Wildom [39]. Applying the procedure to (3.19), we get

$$\mathbb{P}[\lambda_1^{(1)} \le s_1,\ldots,\lambda_1^{(M)} \le s_M] = \det[1 + K_g], \tag{3.22}$$

where $g(t_j,x) = -\chi_{(s_j,\infty)}(x)$. The kernel is

$$K(t_r,x;t_s,y) = K'(t_r,x;t_s,y) - \phi(t_r,x;t_s,y), \tag{3.23}$$

where

$$K'(t_r,x;t_s,y) = \sum_{j,k=0}^{N-1} \Psi_j(x,t_r;t_M)(A^{-1})_{j,k}\Phi_k(t_0;t_s,y), \tag{3.24}$$

$$\Psi_j(x,t_r;t_M) = \int_{-\infty}^{\infty} \phi(t_r,x;t_M,y)y^j dy, \tag{3.25}$$

$$\Phi_j(0;t_s,y) = \int_{-\infty}^{\infty} e^{\epsilon_j+1^x} e^{-x^2} \phi(0,x;t_s,y)dx, \tag{3.26}$$

$$A_{j,k} = \int_{-\infty}^{\infty} dx\, dy\, e^{\epsilon_{j+1}x} e^{-x^2} \phi(0,x;t_M,y)y^k. \tag{3.27}$$

The analysis of the kernel using above equations seems to be difficult since (3.24) involves the inverse matrix. However, we can tackle this difficulty by improving the method of orthogonal polynomial in RMT [40]. We use efficiently the degree of freedom that the value of a determinant is unchanged by elementary transformations. Let us define $F_{k,\epsilon}(x)$ by

$$F_{k,\epsilon}(x) = k!2^{k/2} \int_{\Gamma(\epsilon')} \frac{dz}{2\pi i} \frac{e^{-z^2/2+\sqrt{2}zx}}{\prod_{l=1}^{k+1}(z-\epsilon_l')}, \tag{3.28}$$

where $\Gamma(\epsilon')$ represents the contours enclosing all points $\epsilon_l'(l=1,\ldots,k+1)$ anticlockwise. We also define $G_{k,\epsilon}(x)$ by

$$G_{k,\epsilon}(x) = \frac{2^{k/2}}{\sqrt{2\pi i}} e^{x^2} \int_{\gamma} dw\, e^{w^2/2-\sqrt{2}wx} \prod_{l=1}^{k}(w-\epsilon_l'), \tag{3.29}$$

where $\epsilon_l' = \epsilon_l/\sqrt{2}(l=1,\ldots,N)$ and γ represents an arbitrary path running from $-i\infty$ to $i\infty$. The representations of $F_{j,\epsilon}(x)$ and $G_{j,\epsilon}(x)$ in (3.28) and (3.29) corresponds to the multiple Hermite polynomial of type I and II respectively discussed in [28] except some prefactors. Note that when $\epsilon_i=0$, both (3.28) and (3.29) become the integral representation of the Hermite polynomial with degree k.

One can easily check that $F_k(x)$'s (G_k's) are linear combinations of $e^{\epsilon_k x}$'s (x^k's). Hence one finds

$$\det[e^{\epsilon_j \lambda_k^{(1)}}]_{j,k=1}^{N} = \text{const} \times \det[F_{j,\epsilon}(\lambda_k^{(1)})]_{k=1,\ldots,N}^{j=0,\ldots,N-1}, \tag{3.30}$$

$$\det[(\lambda_j^{(M)})^k]_{k=0,\ldots,N-1}^{j=1,\ldots,N} = \text{const} \times \det[G_{k,e^{-t_M}\epsilon}(\lambda_j^{(M)})]_{k=0,\ldots,N-1}^{j=1,\ldots,N}. \tag{3.31}$$

Applying the same procedure as above, one can show that the operator K on the right hand side in (3.21) can be replaced by another operator $\tilde{K}$, with the kernel $\tilde{K}(t_r,x;t_s,y)$,

$$\tilde{K}(t_r,x;t_s,y) = \tilde{K}'(t_r,x;t_s,y) - \phi(t_r,x;t_s,y), \tag{3.32}$$

where

$$\tilde{K}'(t_r,x;t_s,y) = \sum_{j,k=0}^{N-1} \tilde{\Psi}_j(x,t_r;t_M)(\tilde{A}^{-1})_{j,k}\tilde{\Phi}_k(0;t_s,y), \tag{3.33}$$

$$\tilde{\Phi}_j(0;t_s,y) = \int_{-\infty}^{\infty} F_{j,\epsilon}(x)e^{-x^2}\phi(0,x;t_s,y)dx, \tag{3.34}$$

$$\tilde{\Psi}_j(x,t_r;t_M) = \int_{-\infty}^{\infty} \phi(t_r,x;t_M,y)G_{j,e^{-t_M}\epsilon}(y)dy, \tag{3.35}$$

$$\tilde{A}_{j,k} = \int_{-\infty}^{\infty} dx\, dy\, F_{j,\epsilon}(x)e^{-x^2}\phi(0,x;t_M,y)G_{k,e^{-t_M}\epsilon}(y). \tag{3.36}$$

Substituting (3.20), (3.28), and (3.29) into these equations, we get

$$\tilde{\Phi}_j(0;t_s,y) = e^{-(j+1/2)t_s}e^{-y^2}F_{j,e^{-t_s}\epsilon}(y), \tag{3.37}$$

$$\tilde{\Psi}_j(x,t_r;t_M) = e^{-(j+1/2)(t_M-t_r)}G_{j,e^{-t_r}\epsilon}(x), \tag{3.38}$$

and

$$\begin{aligned}\tilde{A}_{j,k} &= e^{-(j+1/2)t_M}\int_{-\infty}^{\infty} dx\, F_{j,\epsilon}(x)G_{k,\epsilon}(x)e^{-x^2} \\ &= e^{-(j+1/2)t_M}\sqrt{\pi}2^j j!\,\delta_{j,k}.\end{aligned} \tag{3.39}$$

We chose F and G in such a way that $\tilde{A}_{j,k}$ becomes diagonal and can hence be easily invertible. Note that when $\epsilon_i=0$ and $t_M=0$, (3.39) represents the orthogonality of the Hermite polynomials. Our treatment here generalizes the method of orthogonal polynomials for the mutimatrix model between GUE [41,42] to the case with an external source.

Substituting (3.37)–(3.39) to (3.33), one gets

$$\begin{aligned}\tilde{K}'(t_r,x;t_s,y) &= \sum_{j=0}^{N-1} \frac{e^{(j+1/2)t_M}}{\sqrt{\pi}2^j j!}\tilde{\Psi}_j(x,t_r;t_M)\tilde{\Phi}_j(0;t_s,y) \\ &= e^{-y^2}\sum_{j=0}^{N-1} G_{j,e^{-t_r}\epsilon}(x)F_{j,e^{-t_s}\epsilon}(y)e^{-(j+1/2)(t_s-t_r)} \\ &= e^{x^2-y^2}\frac{\sqrt{2}e^{(1/2)(t_r+t_s)}}{(2\pi i)^2}\int_{\Gamma(e^{-t_s}\epsilon')} dz \\ &\quad \times \int_{\gamma} dw e^{w^2/2-\sqrt{2}wx-z^2/2+\sqrt{2}zy} \sum_{j=0}^{N-1} \frac{\prod_{l=1}^{j} e^{t_r}w-\epsilon_l'}{\prod_{l=1}^{j+1} e^{t_s}z-\epsilon_l'},\end{aligned} \tag{3.40}$$

where in the last equality we use (3.28) and (3.29). The summation term in the integrand can be deformed to

$$\sum_{j=0}^{N-1} \frac{\prod_{l=1}^{j} e^{t_r w} - \epsilon_l'}{\prod_{l=1}^{j+1} e^{t_s z} - \epsilon_l'} = \prod_{l=1}^{N} \left(\frac{e^{t_r w} - \epsilon_l'}{e^{t_s z} - \epsilon_l'} \right) \left\{ \frac{1}{e^{t_r w} - \epsilon_N'} \right.$$

$$+ \frac{e^{t_s z} - \epsilon_N'}{(e^{t_r w} - \epsilon_{N-1}')(e^{t_r w} - \epsilon_N')} + \cdots$$

$$\left. + \frac{(e^{t_s z} - \epsilon_2') \cdots (e^{t_s z} - \epsilon_N')}{(e^{t_r w} - \epsilon_1') \cdots (e^{t_r w} - \epsilon_N')} \right\}$$

$$= \prod_{l=1}^{N} \left(\frac{e^{t_r w} - \epsilon_l'}{e^{t_s z} - \epsilon_l'} \right) \left\{ \frac{1}{e^{t_r w} - e^{t_s z}} \right.$$

$$\left. - \prod_{l=1}^{N} \left(\frac{e^{t_s z} - \epsilon_l'}{e^{t_r w} - \epsilon_l'} \right) \frac{1}{e^{t_r w} - e^{t_s z}} \right\}. \tag{3.41}$$

From (3.40) and (3.41) one finally finds the double integral formula of the kernel,

$$\widetilde{K}'(t_r,x;t_s,y) = e^{x^2-y^2} \frac{\sqrt{2} e^{(1/2)(t_r-t_s)}}{(2\pi i)^2} \int_{\Gamma(e^{-t_s}\epsilon')} dz \int_{\gamma} dw$$

$$\times \prod_{l=1}^{N} \frac{e^{t_r w} - \epsilon_l/\sqrt{2}}{e^{t_s z} - \epsilon_l/\sqrt{2}} \frac{1}{w e^{t_r - t_s} - z}$$

$$\times e^{w^2/2 - \sqrt{2} w x - z^2/2 + \sqrt{2} z y}, \tag{3.42}$$

where we use the fact that the second term in (3.41) does not contribute to the double integral in (3.40). In the one matrix case where $t_r = t_s$, the kernel in (3.42), becomes equivalent to the kernel (2.20) obtained by Brézin-Hikami except the prefector irrelevant for the determinant.

D. GOE^2-GUE transition

We consider the asymptotic form of the kernel (3.23) under the edge scaling. Hereafter we consider the case where $\epsilon_1 = \epsilon$, $\epsilon_j = 0 (j = 2, \ldots, N)$. Rescaling the integration variables w, z, the kernel (3.42) is rewritten as

$$\widetilde{K}'(t_1,x;t_2,y) = e^{x^2-y^2} \frac{\sqrt{2N} e^{(1/2)(t_1-t_2)}}{(2\pi i)^2} e^{(N-1)(t_1-t_2)}$$

$$\times \int_{\Gamma_N'} dz \int_{\gamma} dw \frac{z}{w} \frac{e^{t_1 w} - \epsilon/\sqrt{2N}}{e^{t_2 z} - \epsilon/\sqrt{2N}} \frac{1}{w e^{t_1 - t_2} - z}$$

$$\times \frac{e^{\sqrt{2N} z y - 2Nz}}{e^{\sqrt{2N} w x - 2Nw}} e^{N\{f(w) - f(z)\}}, \tag{3.43}$$

where the contour Γ_N' encloses the origin and $e^{-t_2}\epsilon'/\sqrt{N}$ counterclockwise and

$$f(w) \equiv \frac{w^2}{2} - 2w + \ln w. \tag{3.44}$$

We analyze the asymptotic behavior of (3.43) by applying the saddle point method. We scale the variables in (3.43) as

$$x = \sqrt{2N} + \frac{\xi_1}{\sqrt{2} N^{1/6}}, \quad y = \sqrt{2N} + \frac{\xi_2}{\sqrt{2} N^{1/6}},$$

$$t_1 = \frac{\tau_1}{N^{1/3}}, \quad t_2 = \frac{\tau_2}{N^{1/3}},$$

$$\epsilon = \sqrt{2N} \left(1 - \frac{\omega}{N^{1/3}} \right). \tag{3.45}$$

The critical point of the function $f(w)$,

$$w_c = 1, \tag{3.46}$$

turns out to be the double critical point,

$$f'(w_c) = f''(w_c) = 0. \tag{3.47}$$

Thus by deforming the paths of the integration in (3.43) in a way that they cross the critical point,

$$w = 1 - \frac{i w_1}{N^{1/3}}, \tag{3.48}$$

$$z = 1 + \frac{i w_2}{N^{1/3}}, \tag{3.49}$$

we get

$$e^{N\{f(w) - f(z)\}} \sim e^{(i/3)(w_1^3 + w_2^3)}, \tag{3.50}$$

where we use

$$f(w) \sim f(w_c) + f'(w_c)(w - w_c) + \frac{f''(w_c)}{2!}(w - w_c)^2$$

$$+ \frac{f'''(w_c)}{3!}(w - w_c)^3 = \frac{-3}{2} + \frac{i}{3N} w_1^3. \tag{3.51}$$

For other terms in (3.43) we obtain the asymptotic forms under the scaling (3.45),

$$\frac{e^{t_1 w} - \epsilon/\sqrt{2N}}{e^{t_2 z} - \epsilon/\sqrt{2N}} \sim \frac{\tau_1 + \omega - i w_1}{\tau_2 + \omega + i w_2}, \tag{3.52}$$

$$\frac{1}{w e^{t_1 - t_2} - z} \sim - \frac{N^{1/3}}{\tau_2 - \tau_1 + i w_1 + i w_2}, \tag{3.53}$$

$$\frac{e^{\sqrt{2N} z y - 2Nz}}{e^{\sqrt{2N} w x - 2Nw}} \sim e^{N^{1/3}(\xi_2 - \xi_1) + i \xi_1 w_1 + i \xi_2 w_2}, \tag{3.54}$$

$$e^{x^2 - y^2 + (1/2)(t_1 - t_2) + (N-1)(t_1 - t_2)} \sim e^{2N^{1/3}(\xi_1 - \xi_2) + N^{2/3}(\tau_1 - \tau_2)}. \tag{3.55}$$

Hence we eventually find

$$\begin{aligned}\widetilde{K}' &\sim \sqrt{2}N^{1/6}e^{N^{2/3}(\tau_1-\tau_2)+N^{1/3}(\xi_1-\xi_2)} \\ &\times \int_{-\infty}^{\infty}\frac{dw_1}{2\pi}\int_{-\infty}^{\infty}\frac{dw_2}{2\pi}\left(-\frac{1}{\tau_2-\tau_1+i(w_1+w_2)}\right. \\ &\left.+\frac{1}{\omega+\tau_2+iw_2}\right)e^{i(\xi_1w_1+\xi_2w_2)+(i/3)(w_1^3+w_2^3)} \\ &= \sqrt{2}N^{1/6}e^{N^{2/3}(\tau_1-\tau_2)+N^{1/3}(\xi_1-\xi_2)} \\ &\times\left\{\int_0^{\infty}d\lambda\, e^{-\lambda(\tau_1-\tau_2)}\mathrm{Ai}(\xi_1+\lambda)\mathrm{Ai}(\xi_2+\lambda)\right. \\ &\left.+\mathrm{Ai}(\xi_1)\int_0^{\infty}d\lambda\, e^{-(\omega+\tau_2)\lambda}\mathrm{Ai}(\xi_2-\lambda)\right\}, \end{aligned} \tag{3.56}$$

where we use the integral representation of the Airy function,

$$\mathrm{Ai}(x)=\int_{-\infty}^{\infty}d\lambda\, e^{i\lambda x+(i/3)\lambda^3}. \tag{3.57}$$

It is also necessary to consider the asymptotics of $\phi(t_1,x;t_2,y)$ in (3.20) under the same scaling as in (3.45). One has

$$\begin{aligned}-\frac{1}{1-e^{2(t_1-t_2)}} &\sim \frac{N^{1/3}}{2(\tau_2-\tau_1)}\left\{1+\frac{1}{N^{1/3}}(\tau_2-\tau_1)\right. \\ &\left.+\frac{1}{3N^{2/3}}(\tau_2-\tau_1)^2+\cdots\right\}, \\ (e^{t_1-t_2}x-y)^2 &\sim 2N^{1/3}\left\{(\tau_2-\tau_1)^2-\frac{1}{N^{1/3}}(\tau_2-t_1)^3\right. \\ &+\frac{1}{N^{1/3}}(\xi_2-\xi_1)(\tau_2-\tau_1) \\ &-\frac{1}{2N^{2/3}}(\xi_2-\xi_1)(\tau_2-\tau_1)^2+\frac{7}{12N^{2/3}}(\tau_2-\tau_1)^4 \\ &\left.+\frac{1}{4N^{2/3}}(\xi_2-\xi_1)^2+\frac{\xi_1}{N^{2/3}}(\tau_2-\tau_1)^2\right\}. \end{aligned} \tag{3.58}$$

Substituting these into (3.20), one gets

$$\phi\sim\begin{cases}\sqrt{2}N^{1/6}e^{N^{2/3}(\tau_1-\tau_2)+N^{1/3}(\xi_1-\xi_2)}\displaystyle\int_{-\infty}^{\infty}d\lambda\, e^{-\lambda(\tau_1-\tau_2)}\mathrm{Ai}(\xi_1+\lambda)\mathrm{Ai}(\xi_2+\lambda) & \text{for } \tau_1\leqslant\tau_2, \\ 0 & \text{for } \tau_1>\tau_2.\end{cases} \tag{3.59}$$

Thus we finally find

$$\sqrt{2}N^{1/6}\widetilde{K}\to e^{N^{2/3}(\tau_1-\tau_2)+N^{1/3}(\xi_1-\xi_2)}\mathcal{K}(\tau_1,\xi_1;\tau_2,\xi_2), \tag{3.60}$$

where $\mathcal{K}(\tau_1,\xi_1;\tau_2,\xi_2)$ is the same as the one appearing in the analysis of the PNG model with external source (3.4). Since the prefactor is irrelevant to the value of Fredholm determinants, we have shown that the fluctuation of the PNG height described by (3.3)–(3.5) is equivalent to the fluctuation of the largest eigenvalue of the multimatrix model (3.18) with an appropriate choice of V.

IV. CONCLUSION

We have presented a random matrix model with a deterministic source, the largest eigenvalue of which describes the height fluctuations of the PNG model with an external source. Depending on the value of the deterministic source, the distribution of the largest eigenvalue in this model becomes the GUE Tracy-Widom distribution and the GOE^2. It also describes the transition between these two, which could not be understood by the previous interpretation of the GOE^2 as "the square of GOE." Our model gives not only another representation of the GOE^2 but also a unified picture including GUE, GOE^2 and their transition.

We have also considered a vicious walk model which has a similar topology to that of the multilayer PNG model. In an appropriate limit, this leads us to a Dyson's Brownian motion model with a deterministic source as an initial condition. At last we have found the process of the largest eigenvalue in the edge scaling of this model describes the multipoint joint distributions of the PNG model with an external source.

ACKNOWLEDGMENTS

The authors would like to thank M. Katori, T. Nagao, A. Rákos, G. M. Schütz, and H. Spohn for fruitful discussions and comments. The work of T.I. is partly supported by Grant-in-Aid from the Ministry of Education, Culture, Sports, Science and Technology, Japan. The work of T.S. is partly supported by a Grant-in-Aid from the Ministry of Education, Culture, Sports, Science and Technology, Japan.

[1] M. Kardar, G. Parisi, and Y. C. Zhang, Phys. Rev. Lett. **56**, 889 (1986).
[2] M. Prähofer and H. Spohn, Physica A **279**, 342 (2000).
[3] K. Johansson, Commun. Math. Phys. **209**, 437 (2000).
[4] J. Baik, P. Deift, and K. Johansson, J. Am. Math. Soc. **12**, 1119 (1999).
[5] J. Baik and E. M. Rains, Duke Math. J. **109**, 1 (2001).
[6] J. Baik and E. M. Rains, Duke Math. J. **109**, 205 (2001).
[7] J. Baik and E. M. Rains, in *Random Matrix Models and Their Applications* edited by P. M. Bleher and A. R. Its (Cambridge University Press, Cambridge, 2001), pp. 1–29.
[8] C. A. Tracy and H. Widom, Commun. Math. Phys. **159**, 151 (1994).
[9] C. A. Tracy and H. Widom, Commun. Math. Phys. **177**, 727 (1996).
[10] M. Prähofer and H. Spohn, Phys. Rev. Lett. **84**, 4882 (2000).
[11] M. Prähofer and H. Spohn, J. Stat. Phys. **108**, 1071 (2002).
[12] K. Johansson, Commun. Math. Phys. **242**, 277 (2003).
[13] T. Sasamoto and T. Imamura, J. Stat. Phys. **115**, 749 (2004).
[14] J. Baik and E. M. Rains, J. Stat. Phys. **100**, 523 (2000).
[15] M. Prähofer and H. Spohn, in *In and Out of Equilibrium*, edited by V. Sidoravicius, Vol. 51 of Progress in Probability (Birkhauser, Boston, 2002), pp. 185–204.
[16] T. Nagao and T. Sasamoto, Nucl. Phys. B **699**, 487 (2004).
[17] P. J. Forrester, "Painlevé transcendent evaluation of the scaled distribution of the smallest eigenvalue in the Laguerre orthogonal and symplectic ensembles," nlin.SI/0005064.
[18] E. Brézin, S. Hikami, and A. Zee, Phys. Rev. E **51**, 5442 (1995).
[19] E. Brézin and S. Hikami, Phys. Rev. E **55**, 4067 (1997).
[20] E. Brézin and S. Hikami, Phys. Rev. E **56**, 264 (1997).
[21] E. Brézin and S. Hikami, Phys. Rev. E **57**, 4140 (1998).
[22] E. Brézin and S. Hikami, Phys. Rev. E **58**, 7176 (1998).
[23] E. Brézin, S. Hikami, and A. Zee, Nucl. Phys. B **464**, 411 (1996).
[24] E. Brézin and S. Hikami, Nucl. Phys. B **479**, 697 (1996).
[25] P. Zinn-Justin, Nucl. Phys. B **497**, 725 (1997).
[26] P. Zinn-Justin, Commun. Math. Phys. **194**, 631 (1998).
[27] P. M. Bleher and A. B. J. Kuijlaars, Int. Math. Res. Notices **2004**, 109 (2004).
[28] P. M. Bleher and A. B. J. Kuijlaars, "Integral representations for multiple Hermite and multiple Laguerre polynomials," math.CA/0406616.
[29] P. M. Bleher and A. B. J. Kuijlaars, "Large *n* limit of Gaussian random matrices with external source, part I," Commun. Math. Phys. **252**, 43 (2004).
[30] A. I. Aptekarev, P. M. Bleher, and A. B. J. Kuijlaars, "Large *n* limit of Gaussian random matrices with external source, part II," math-ph/0408041.
[31] P. J. Forrester, Nucl. Phys. B **402**, 709 (1994).
[32] J. Baik, G. Ben Arous, and S. Peche, "Phase transition of the largest eigenvalue for non-null complex sample covariance matrices," math.PR/0403022.
[33] T. Imamura and T. Sasamoto, Nucl. Phys. B **699**, 503 (2004).
[34] A. M. S. Macêdo, Europhys. Lett. **26**, 641 (1994).
[35] M. Katori and H. Tanemura, Phys. Rev. E **66**, 011105 (2002).
[36] M. Katori and H. Tanemura, J. Math. Phys. **45**, 3058 (2004).
[37] Harish-Chandra, Am. J. Math. **79**, 87 (1957).
[38] C. Itzykson and J. B. Zuber, J. Math. Phys. **21**, 411 (1980).
[39] C. A. Tracy and H. Widom, J. Stat. Phys. **92**, 809 (1998).
[40] M. L. Mehta, *Random Matrices*, 2nd ed. (Academic, New York, 1991).
[41] B. Eynard and M. L. Mehta, J. Phys. A **31**, 4449 (1998).
[42] P. J. Forrester, T. Nagao, and G. Honner, Nucl. Phys. B **553**, 601 (1999).